Desalination and Water Treatment
www.deswater.com

doi: 10.1080/19443994.2014.940206

55 (2015) 2939–2950
September

Taylor & Francis
Taylor & Francis Group

Improvement of reverse osmosis performance of polyamide thin-film composite membranes using TiO_2 nanoparticles

Abdel-hameed Mostafa A. El-Aassar

Desalination Unit, Hydro-geochemistry Department, Desert Research Center (DRC), Cairo, Egypt, Tel. +20 2 01002501524; Fax: +20 2 26389069; email: hameed_m50@yahoo.com

Received 25 February 2014; Accepted 16 June 2014

ABSTRACT

The present paper explores the role of Titanium dioxide (TiO_2) nanoparticles in the improvement of performance of polyamide thin-film composite reverse osmosis (RO) membranes. It reports on novel PA/TiO_2 thin-film nanocomposite (TFNC) membranes via *in situ* interfacial polymerization technique. It carried out by pre-dispersed TiO_2 nanoparticles in either organic phase (dodecane) of trimesoyl chloride or aqueous phase of *m*-phenylenediamine. The change in chemical and physical properties of the synthesized TFNC membranes was evaluated through studying ATR-FTIR spectroscopy, contact angle measurements, scanning electron microscopy, and X-ray photoelectron spectroscopy. Also, the effect of TiO_2 concentration on RO performance and organic antifouling resistance was investigated. The synthesized PA-TiO_2 TFNC membranes exhibited an improvement in permeate flux which increased from 33.6 to 40 L/m^2h with slightly increase in salt rejection (%) which increased from 99.75 to 99.82%. The synthesized TFNC membrane with low-concentration TiO_2 showed an improvement for the organic fouling resistance. The synthesized PA-TiO_2 TFNC membranes offering a strong potential for possible use as a novel type of TFNC membranes with high RO performance.

Keywords: TiO_2 nanoparticles; Thin-film nanocomposite; *In situ* interfacial polymerization; Reverse osmosis membranes

1. Introduction

In general, desalination technologies can be categorized into two different mechanism separations: thermal and membrane-based desalination. The thermal processes include multi-stage flash, multiple effect distillation, and vapor compression distillation, whereas membrane-based processes include reverse osmosis (RO), nanofiltration, and electrodialysis. Among these technologies, RO membrane desalination is the primary choice where it dominates up to 44% of the total world desalination capacity [1].

Membrane technologies are getting more and more attention nowadays due to their reliable contaminant removal without production of any harmful by-products, especially in water and wastewater treatment processes. Researchers are focusing more on polymeric materials because of better pore-forming control and lower cost [2]. Thin-film composite (TFC) membranes

Presented at the Conference on Desalination for the Environment: Clean Water and Energy 11–15 May 2014, Limassol, Cyprus

are extensively used in RO desalination applications. Since the breakthrough discovery made by Cadotte and his co-workers in the 1970s, TFC membrane prepared using interfacial polymerization (IP) technique has experienced significant progress in composite membrane development and emerged as one of the most advanced technologies in water and wastewater purification processes [3]. In spite of that the most common disadvantage associated with the application of the membrane process in water and wastewater treatment is membrane fouling, which results in flux decline during the operation [4,5]. Some fouling materials even destroy the membrane and shorten its service life. However, membrane material is frequently accepted as one of the predominant fouling modulators, with membrane fouling expected to be more severe with hydrophobic than hydrophilic membranes [6,7].

The main approach toward minimizing polymeric membrane fouling is the prevention of the undesired adsorption or adhesion processes on the surface of the membrane, because this will prevent or, at least, slow down the subsequent accumulation of colloids. Several strategies to alleviate the membrane fouling have been investigated. One of these methods is hydrophilic modification of membrane surface [8]. There are various methods available for hydrophilic modification of membrane surface [9–15]. Among these methods, incorporation of various kinds of nanoparticles into the polymeric membranes has been the focus of numerous investigations in recent years.

The unique chemical and physical properties of nanosized metals as compared with their bulk particles have increased the studies of nanoparticle synthesis for specific optical, magnetic, electronic, and catalytic purposes. Polymeric systems have been used in the preparation of nanoscaled particles due to the presence of specific functional groups on the backbone of the polymer chain. These groups are often ionic in nature or have lone-pair electrons that can be served as a chelating agent as well as imposing a stabilizing effect on the synthesized nanoparticles. A typical nanoparticle containing atoms or molecules numbering from tens to tens of thousands has a length between a few and a few tens of nanometers. The introduced nanoparticles to polymer membranes might be silica [16], Fe_3O_4 [17], ZrO_2 [18], CdS [19], and TiO_2 [20–23].

Titanium dioxide (TiO_2) has received much attention because of its important role in various applications such as photocatalysis, oxygen sensors, antimicrobial coatings, and pigment [24,25]. Among them, the photocatalytic properties to decompose organic compounds can be used in filtration membranes, which possibly overcome the fouling phenomena in the membranes [26–28].

In this study, polyamide thin-film nanocomposite (TFNC) membranes containing TiO_2 nanoparticles were prepared. The PA barrier layer was formed via interfacial (IP) polymerization between *m*-phenylenediamine (MPD) in aqueous solution with trimesoyl chloride (TMC) in dodecane solution. *In situ* IP with TiO_2 occurred by pre-dispersed TiO_2 nanoparticles in either the organic or the aqueous phase. This process is greatly effective in helping the confinement of TiO_2 inside PA polymeric chains. The synthesized membranes have been characterized by ATR-FT-IR spectroscopy, contact angle measurements, scanning electron microscopy (SEM), and X-ray photoelectron spectroscopy (XPS).The membrane RO performance including permeate flux (L/m^2h) and salt rejection (%) as well as organic fouling resistance was evaluated as a function of TiO_2 concentration.

2. Experimental

2.1. Materials and reagents

Asymmetric polysulfone (PS) support membrane cast on polyester non-woven polyester fabric was kindly supplied by Dow Water & Process Solutions (Edina, MN). *m*-phenylenediamine (MPD, ≥ 99%), (TMC, 98%), TiO_2 anatase with particle size < 25 nm, *n*-dodecane (anhydrous, ≥ 99%), and *n*-hexane (mixture of isomers, anhydrous, ≥ 99%) were used as received from Sigma–Aldrich (St. Louis, MO). Deionized (DI) water was generated by a Milli-Q Advantage A10 vacuum purification system (Millipore, Billerica, MA).

Acrylic plastic plates (8 in × 11 in × 0.24 in) were used to support the PS membranes during TFC membranes preparation. Additionally, plastic frames (inner size: 6 in × 9 in) were cut from these plates. Rubber gaskets having the same size of the plastic frames were purchased from Advanced Gasket & Supply (Fort Worth, TX, USA). Soft rubber rollers were purchased from Sigma–Aldrich Co. (St. Louis, MO, USA).

2.2. Preparation of polyamide thin-film (PA-TFC) membranes

The process of membrane preparation is believed to be similar to that reported by Mitchell et al. [29] and Xie et al. [30], as shown in Fig. 1.

PS support membranes were immersed in DI water for 1 h, (Fig. 1(a)) then removed from the DI water and positioned on a plastic plate. A rubber gasket and a plastic frame were placed on top of the PS support

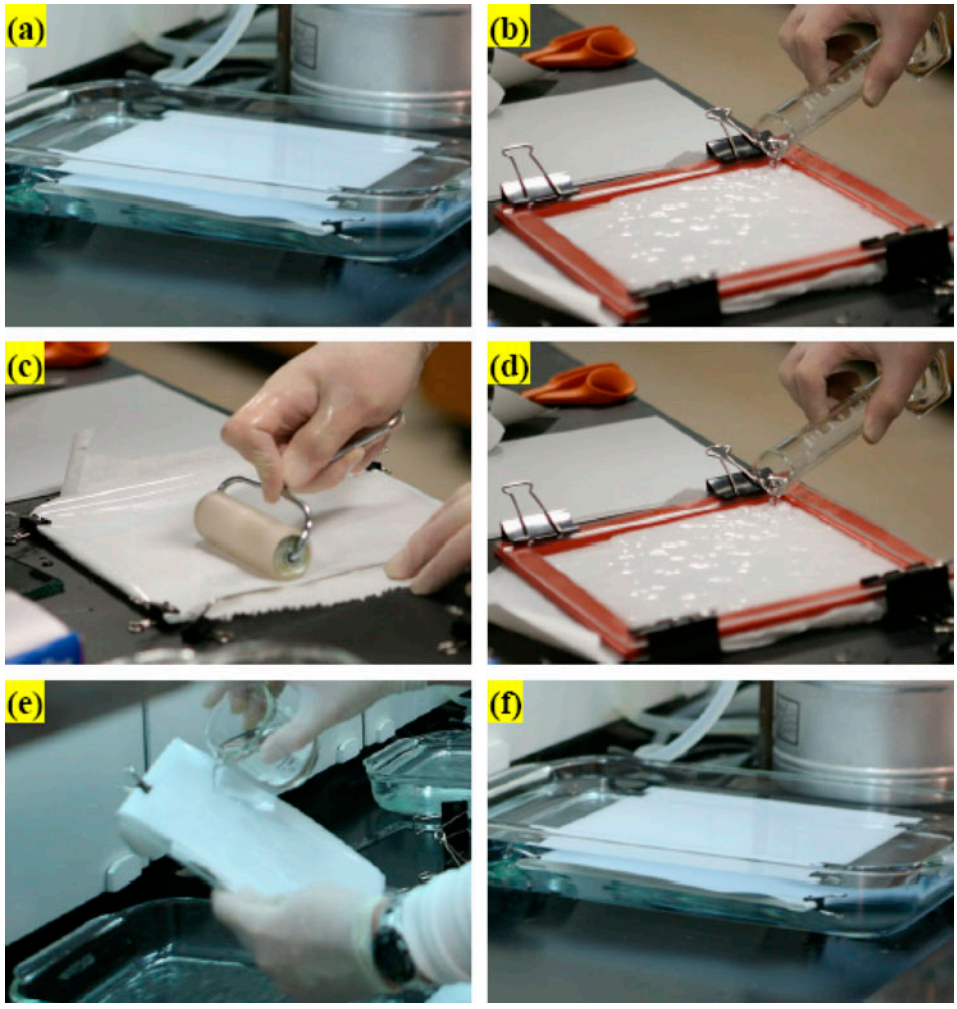

Fig. 1. Protocol to prepare polyamide TFC membranes.

membrane, and binder clips were used to hold the plate-membrane-gasket-frame stack together. MPD aqueous solution with or without TiO_2 nanoparticles was poured onto the frame (Fig. 1(b)) and allowed to contact on the PS membrane for a time before draining the excess MPD solution. This residence time allowed MPD to at least partially penetrate into the pores of the porous PS support layer. The frame and gasket were disassembled and residual solution between the plate and the PS was removed. Residual MPD droplets on the top surface of the PS membrane were removed by firmly pressed rolling a rubber roller across the membrane surface (Fig. 1(c)) for one time and one direction to ensure that there are no visible aqueous droplets, these droplets could form defects if left on the membrane surface. The frame and gasket were reassembled on top of the PS membrane, and the organic solution of TMC (with or without TiO_2 nanoparticles) was poured onto the frame (Fig. 1(d)). It is important to mention that in this study, the dodecane was used as the organic solvent of TMC. After a time, the organic solution was drained from the frame, and the frame and gasket were disassembled. The membrane surface was washed by hexane (Fig. 1(e)) to accelerate the evaporation process and let to dry in air at ambient conditions. Finally, the prepared membrane was immersed in DI water (Fig. 1(f)) until characterized or used in cross-flow experiments.

2.3. Characterization of PA-TFC membranes

Attenuated total reflectance Fourier transform infrared spectroscopy (ATR-FTIR) was used to characterize the chemical structure of the polyamide TFC membranes. A Thermo Nicolet Nexus 470 FTIR with

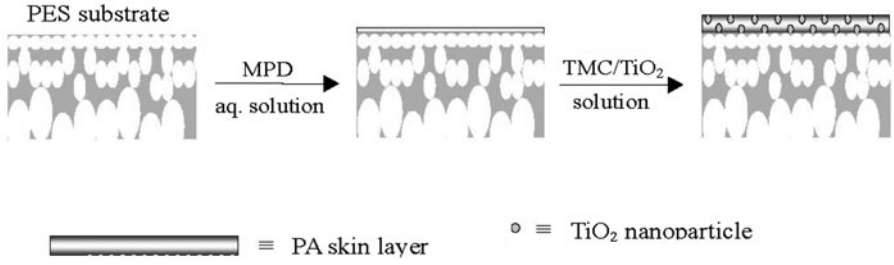

Fig. 2. Preparation procedure for PA-TiO_2 nanocomposite membranes [32].

an Avatar Smart Miracle ATR accessory and a ZnSe crystal (Thermo Fisher Scientific Inc., Waltham, MA) was used. Spectra were collected in air, in the mid-infrared region (600–4,000 cm^{-1}), using 128 scans at resolution 4. After each measurement, a background spectrum was obtained using PS membrane and subtracted from that of the membrane to remove any atmospheric absorbance peaks.

The Oil-in-water contact angle analysis was performed using a Ramé-Hart Model 200-F1 Standard Goniometer with DROP image Standard Edition 2.4 software (Ramé-Hart Instrument Co., Netcong, NJ). A strip of membrane was mounted in a sample holder with polyamide side facing down and was placed in DI water environment. An n-decane oil droplet was dispensed onto the bottom side of the membrane strip from a Gilmont Instruments 0.2 ml micrometer syringe (Cole-Parmer Instrument Co., Vernon Hills, IL) with a hooked Hamilton N732 needle (OD: 0.009 in, Hamilton Co., Reno, NV). Contact angles were measured through the water phase, and the reported contact angle is the average value of the left and right side contact angles, at least three oil droplets placed at different spots in each sample (any membrane was measured using three samples). A smaller angle indicates a more hydrophilic surface.

Also, synthesized membrane surfaces and cross-sections morphology were characterized by scanning electron microscopy (SEM, Zeiss Supra 40 VP, Carl Zeiss NTS, Peabody, MA). High-voltage ETH mode was used and the voltage was set to 5 kv. An In Lens detector was selected, and the working distance was between 5 and 7 mm. Samples were prepared by peeling away the non-woven polyester backing fabric and fracturing the remaining PS and polyamide layers after immersion in liquid nitrogen. A Cressington 208 Bench-top Sputter Coater (Cressington Scientific Instruments Ltd., Watford, England) having a pt/pd metal target was used to coat the samples. The coating thickness was set 10 nm to ensure adequate sample surface conductivity.

XPS was used to characterize the surface elemental content of modified and unmodified membranes. XPS probes a maximum depth of ~10 nm (at 0˚ takeoff angle i.e. perpendicular to the membrane surface), making it a better choice than ATR-FTIR for detection of the polyamide layer (~0.1 μm) and any surface changes effected by PEGDE grafting. Surface scans were performed using an AXIS Ultra DLD XPS (Kratos Analytical Company, Chestnut Ridge, NY) equipped with a monochromatic Al Kα1,2 X-ray source (2×10^{-9} Torr chamber pressure, 15 kV, 150 W). Carbon (1s), nitrogen (1s), oxygen (1s), and sulfur (2p) were detected using either a 0˚ or 45˚ takeoff angle (to probe an even thinner surface layer). A 300 μm × 700 μm area was analyzed, and a charge neutralizer was used to minimize sample charging.

2.4. RO performance of PA-TFC membranes

The RO performance of the prepared PA-TFC membranes was evaluated through measuring both permeate flux (L/m^2 h) and salt rejection (%). Permeate flux and salt rejection were measured using cross-flow filtration using aqueous feed solution contained 2,000 ppm NaCl with pH range 7 ± 0.3 samples at 25˚C. The flow rate was 1gallon per minute and the applied pressure was 225 psi (15.5 bar). All flux and rejection measurements were evaluated after 30 min from the starting of the cross-flow experiment to ensure that the filtration process had reached steady state.

The permeate flux (J_W) through a membrane area (A) was calculated as the volume (ΔV) collected during a time period Δt:

$$J_W = \Delta V/A \times \Delta t$$

Also, the salt rejection (R_s %) was calculated by measuring the electric conductivity of both feed and permeate solutions using an Oakton CON 11 conductivity meter (cole-Parmer Instrument Co., Vernon Hills, IL).

The salt rejection percent (R_s %) was calculated as follows:

$$R_s\ \% = (C_f - C_p/C_f) \times 100$$

where C_f and C_p are the concentrations of the feed and permeate water (product), respectively.

2.5. Antifouling resistance tests of synthesized membranes

Oil fouling experiments were performed using a feed of oil-in-water emulsion after using both pure and 2,000 ppm NaCl aqueous solution in the cross-flow filtration system. The cross-flow system was cleaned before each experiment as the previous work [31]. The feed for the oily water tests consisted of 30 L of oil-in-water emulsion containing 1,500 ppm soybean oil emulsion (9:1 of oil: DC193C ratio), i.e. 40.5 g of soybean oil and 4.5 g of DC193C. (From Dow Co.), which had been freshly prepared by blending appropriate amounts of oil, surfactant, and water for 3 min at 20,000 rpm in a 3 L blender (Waring LBC15, Waring Laboratory & Science, Torrington, CT). During the fouling test, the permeate from each membrane was collected in a beaker placed on a balance connected to a LabVIEW data acquisition program (National Instruments Co., Austin, TX) for continuous monitoring of permeate mass. These data were used to calculate flux as a function of the time that the membranes were in contact with the oil/water emulsion.

3. Results and discussion

Many experiments for PA-TiO_2 membranes had been reported previously [21,32]. In the first study [21], the PA-TiO_2 membranes were prepared using *ex situ* by dipping the prepared PA-TFC in TiO_2 colloidal solution for a certain time to deposit TiO_2 nanoparticles on the membrane surface. However, that method is vulnerable to easier detachment of TiO_2 from the PA matrix, leading to the decrease of TiO_2 concentration in the membranes. While in the other study [32], TiO_2 nanoparticles were homogeneously dispersed in the organic phase of TMC solution. The *in situ* IP reaction may produce the confinement of TiO_2 nanoparticles on both the surface and inside the PA membrane. The procedure for the preparation of PA-TiO_2 nanocomposite membranes is illustrated in Fig. 2. In spite of it provides higher concentration of TiO_2 nanoparticles in the membranes and more robust structure of PA-TiO_2 nanocomposite membranes but it did not improve the RO performance significantly and any increase in the flux accompanied a decrease in salt rejection.

3.1. Synthesis and characterization of PA-TiO_2 TFNC membranes

In the present work, TiO_2 nanoparticles with different concentrations were homogeneously dispersed in either organic or aqueous phase of TMC and MPD, respectively. In organic phase, the TiO_2 concentration ranged from 10 to 100% related to TMC concentration (0.05wt.%), while in case of aqueous phase, TiO_2 concentration ranged from 0.5 to 2% related to MPD concentration (1.5wt.%). The advantages of using these low TiO_2 concentrations are decreasing the possibilities of the nanoparticles aggregation and possessing high specific surface area of TiO_2 nanoparticles. Also, in higher concentration of TiO_2, the mechanical strength of the membranes decreased significantly, producing easier peeling off of the PA-TiO_2 layer from the support layer after the filtration experiment [32].

The synthesized PA/TFC and PA-TiO_2/TFNC membranes were characterized by ATR-FTIR spectroscopy, as shown in Fig. 3. Because the depth of ATR-FTIR penetration was about 0.4–0.5 μm in the wavelength region of interest, the ATR-FTIR spectra reflect a combination of polyamide barrier layer (0.1–0.15 μm) and the rest of the PS substrate (Fig. 3(a)). The spectra of TFC membrane (Fig. 3(b)) shows the absence of the acid chloride band at 1770 cm^{-1}, indicating successful polymerization. The strong bands at 1,661 and 1,549 cm^{-1} were present that it is a characteristic of (amide I) CO

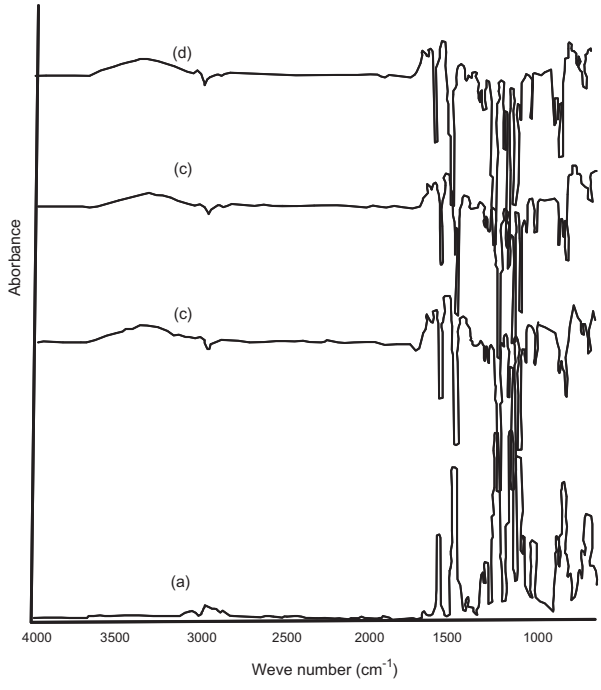

Fig. 3. ATR-RTIR of (a) PS, (b) neat PA-TFC, 20% TiO_2-PA-TFNC in organic phase (c), and in aqueous phase (d).

stretching vibrations and amide-II (N–H) band of amide group (–CONH–). In addition, other bands characteristic of PA occur at 1,609.6 and 1,488.9 cm^{-1} (aromatic ring breathing), and 1,250 cm^{-1} (amide III). Also, the stretching peak of OH group was present at 3,384 cm^{-1}. In addition of TiO_2, in either organic or aqueous phase (Fig. 3(c) and (d)), a small peak due to its low concentration was observed at 755 cm^{-1}, this result was agreement with the previous work [33].

Membrane surface hydrophilicity was characterized in terms of contact angle, and the results are recorded in Table 1. It is obvious that all synthesized TFC membranes possesses good hydrophilicity and the contact angle ranged from 23.1 to 33 ± 2. The addition of TiO_2 nanoparticles in organic phase increased the hydrophilicity, i.e. decreasing the contact angle, up to 40 wt. % of TMC concentration. Further increase of TiO_2 results in a decrease the hydrophilicity. This is due to the possible aggregation of TiO_2 particles and the reaction between the TiO_2 nanoparticles and carboxylic groups leading to decrease the number of free carboxylic groups, as shown in Fig. 4.

Also, in case of addition of TiO_2 in aqueous phase, it increased the hydrophilicity, i.e. decrease the contact angle as compared with neat PA-TFC.

The surfaces and cross-sections of PSF, PA-TFC, and PA-TiO_2 TFNC membranes were imaged by SEM, as shown in Fig. 5. Unlike the smooth and featureless of porous PSf support layer surface, the polyamide PA-TFC surface had a layer of tightly packed globules and scattered ear-shaped polyamide ridges. In case of PA-TiO_2 TFNC membranes, TiO_2 nanoparticles were well dispersed in the membrane surface and increase its roughness. In high concentration of TiO_2, the aggregation of TiO_2 particles was observed in case of doping the TiO_2 nanoparticles in organic phase.

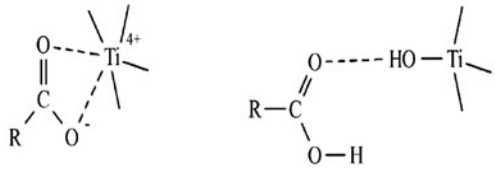

Fig. 4. The mechanism of the reaction between TiO_2 and carboxylic group (by bidendate coordination or by formation H-bond).

Also, the chemical composition of both PA-TFC and PA-TiO_2 TFNC synthesized membranes was analyzed by XPS.

The XPS spectra of neat PA-TFC membrane resulted in typical C1s (284.14 eV), N 1s (399.03 eV), and O 1s (532.11 eV) core levels for aromatic rings, amide groups, and carboxylic acids, as shown in Fig. 6. The spectra are slightly similar to those in the literatures [31,32]. Also, the XPS spectra of TiO_2 PA-TFNC membranes showed the peaks of C1s at (283.93 eV), N 1s at (398.97 eV), and O 1s at (531.83 eV). The photoelectron peak for Ti atom appears clearly at 455 eV for $2p_{2/3}$ and 461 eV for $2p_{1/2}$ as presented in Fig. 7.

3.2. RO performance

RO performance data including permeate flux ($L/m^2 h$) and salt rejection (%) for the synthesized neat PA/TFC and TiO_2-PA/TFNC membranes were studied to evaluate the effect of TiO_2 concentration. Introduction of TiO_2 nanoparticles into either organic or aqueous phase was evaluated to optimize the preparation condition and obtain a membrane with optimal performance characteristics.

Table 1
Effect of TiO_2 addition in either organic or aqueous phase on the contact angle

MPD conc. (wt.%)	TMC (conc.) (wt.%)	TiO_2 (conc.) (%)	Phase	Contact angle
1.5	0.05	–	–	33 ± 2
1.5	0.05	0.005 (10%)	Organic	23.5 ± 2
		0.01 (20%)		23.3 ± 2
		0.02 (40%)		23.1 ± 2
		0.04 (80%)		27.7 ± 2
		0.05 (100%)		29.5 ± 2
1.5	0.055	0.04		24 ± 2
1.5	0.05	0.0075(0.5%)	Aqueous	29.2 ± 2
		0.015(1%)		30.6 ± 2
		0.03(2%)		24.5 ± 2
1.507	0.05	0.015		24.8 ± 2
1.515				25.8 ± 1
1.53				26.1 ± 2

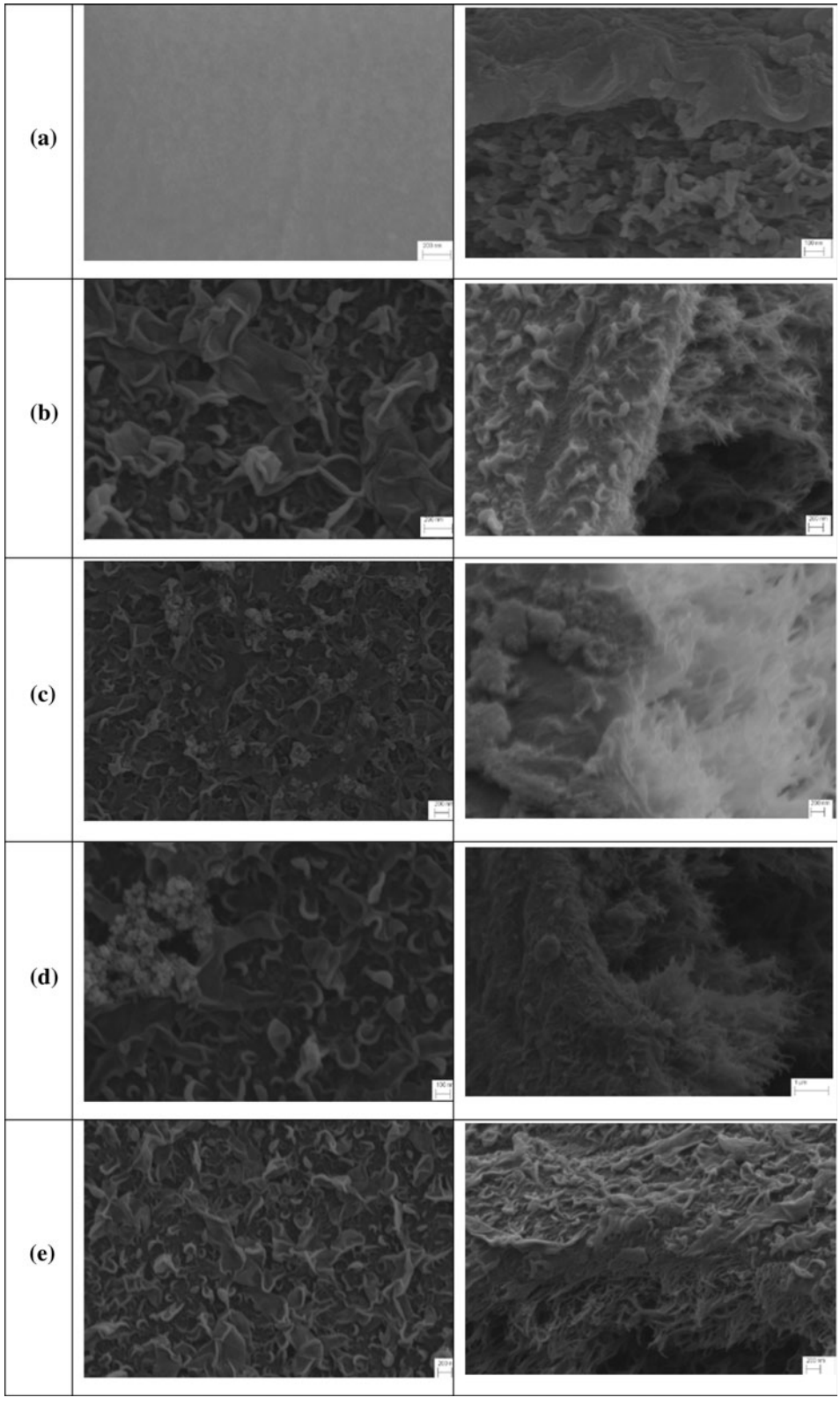

Fig. 5. SEM of (a) PS, (b) Neat PA-TFC, (c) 20%, (d) 80% TiO_2-PA-TFNC in organic phase, and (e) 20% TiO_2-PA-TFNC in aqueous phase.

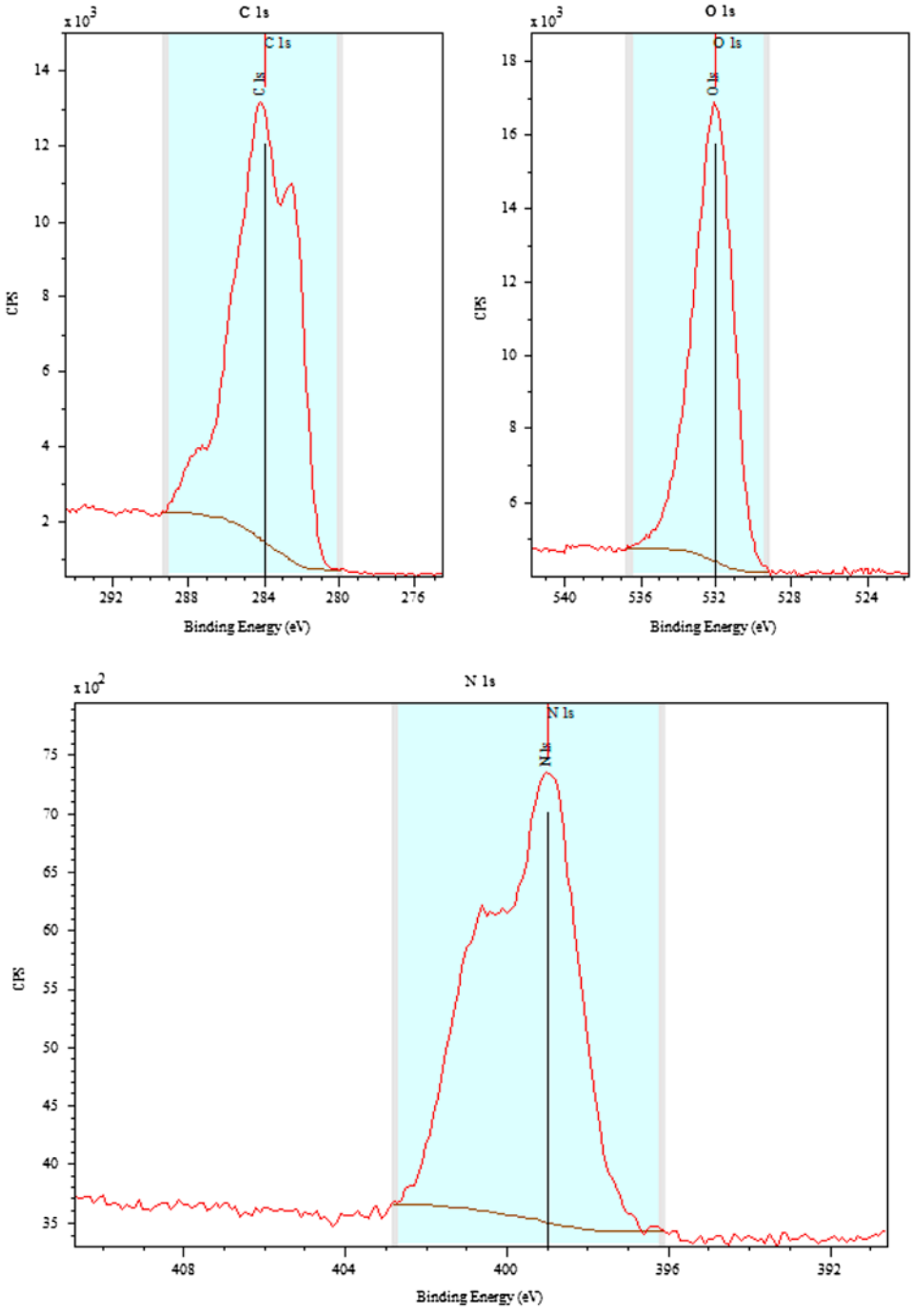

Fig. 6. XPS spectra for carbon, oxygen, and nitrogen for neat PA-TFC membranes.

It is important to mention that the functional groups of the membrane surface play an important role in RO performance [34]. Reid and Breton [35] explained the water permeation in RO membranes by a hydrogen bond formation with functional groups of membrane surface and a formation of bound water. The bound water passes through membrane from one hydrogen-bonding site to another site in the membrane matrix under a pressure gradient, and the passage of a solute component that does not form a hydrogen bond is resisted. Interaction energy and stability of hydrogen-bonding formation between water and membrane surface would have an important effect on water permeability and salt rejection. Water

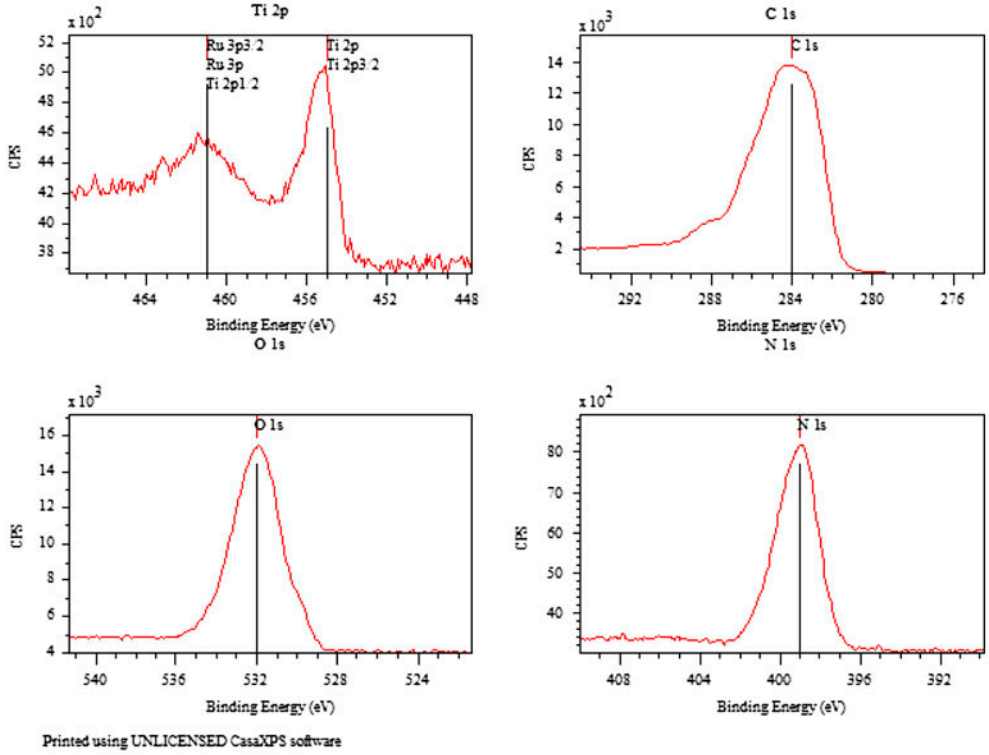

Fig. 7. XPS spectra for carbon, oxygen, nitrogen, and titanium for PA-TiO_2 TFNC membranes.

can form hydrogen bonds with hydrophilic carboxylic acid groups or amide linkages. Both carboxylic acid group and amide functionality yield a shorter and stronger H-bond with water. According to experimental and theoretical results, the doubly bonded oxygen acts as a much more effective proton acceptor than that does hydroxyl oxygen of carboxylic acid and NH group of amide linkage. Moreover, carboxylic acid groups form a slightly more stable and strong H-bond with water than hydrophilic amide groups [36]. Higher stability of H-bond of carboxylic acid group with water would promise a more selective permeation but act as a resistance of the passage of the bound water from one site to another.

The effect of TiO_2 concentration in organic phase on the RO performance of synthesized membranes was shown in Table 2. It is obvious that the best concentration of TiO_2 which improved the performance

Table 2
Effect of TiO_2 concentration (in organic phase) on membrane performance

No.	TiO_2 Conc. (%)	MPD Conc.	TMC Conc.	R_S (%)	J_{H2O} (L/m^2 h)
1	0	1.5	0.05	99.75	33.61
2	10	1.5	0.05	99.75	31.22
3	20	1.5	0.05	99.77	38.78
4	40	1.5	0.05	99.82	36
5	80	1.5	0.05	99.82	34.6
6	100	1.5	0.05	99.86	31.26
7	10	1.4965	0.05	99.82	31.56
8	20	1.493	0.05	99.83	37.55
9	40	1.4863	0.05	99.8	36.73
10	60	1.4795	0.05	99.84	37.32
11	80	1.4728	0.05	99.83	39.6
12	100	1.466	0.05	99.74	24.66

Table 3
Effect of TiO_2 concentration (in aqueous phase) on membrane performance

No.	TiO_2 (%) of MPD	MPD Conc. (%)	R_S (%)	J_{H2O} (L/m^2 h)
1	0	1.5	99.75	33.61
20	0.5	1.5	99.59	33.76
21	1	1.5	99.74	36.56
22	2	1.5	99.52	33.77
21	1	1.5	99.74	36.56
23	1	1.5075	99.58	32.79
24	1	1.515	99.72	40.16
25	1	1.53	99.67	35.35

was (20% of TMC) the flux increased from 33.61 to 38.78 (L/m^2 h) with slightly the same of salt rejection (%). This could be due to the increase of water uptake in the membranes, which comes from the increase of membrane hydrophilicity (see Table 1). Further increasing the TiO_2 concentration leads to a decrease in water flux again with slightly increase in salt rejection (%), this is due to the decrease of free carboxylic group's number and the effect on the NH_2/COCl molar ratio.

So another series of TFNC membranes was prepared using a decreasing concentration of MPD with increasing TiO_2 concentration to maintain the NH_2/COCl molar ratio. It was found that the water flux increase with no significant effect of salt rejection (%) by increasing the TiO_2 concentration up (80% of TMC) which considered the suitable concentration of TiO_2, it improved the water flux from 33.6 to 39.6 (L/m^2 h) with slightly improved in salt rejection which increase from 99.75 to 99.83 (%). Further increasing in TiO_2 concentration, abruptly decrease in water flux was obtained.

Also, the introduction of TiO_2 in MPD aqueous phase was studied, as shown in Table 3. It is obvious that as TiO_2 increase the water flux improved with slightly the same of salt rejection up to 1 wt. % of MPD concentration. After that any increase leads to a decrease in water flux. This may be due to the effect on the value of NH_2/COCl molar ratio.

So another series of TFNC membranes was prepared using an increasing of MPD concentration. It is obvious that the best concentration of MPD (1.515 wt. %) which improved the flux was increased from 33.6 to 40.16 (L/m^2 h) with slight effect in salt rejection.

3.3. Organic antifouling resistance evaluation

The permeation and separation performance of composite membranes were evaluated by cross-flow filtration system using 1500 ppm soybean oil emulsion.

Fig. 8 presents the permeate flux for three selected membranes (Neat PA-TFC, 20%and 80% TiO_2-PA/TFNC membranes) as a function of operation time, where the three selected membranes were tested side by side using pure, saline, and oil emulsion solution. After 25 h, all synthesized composite membranes exhibited good fouling resistance and the PA-TFNC

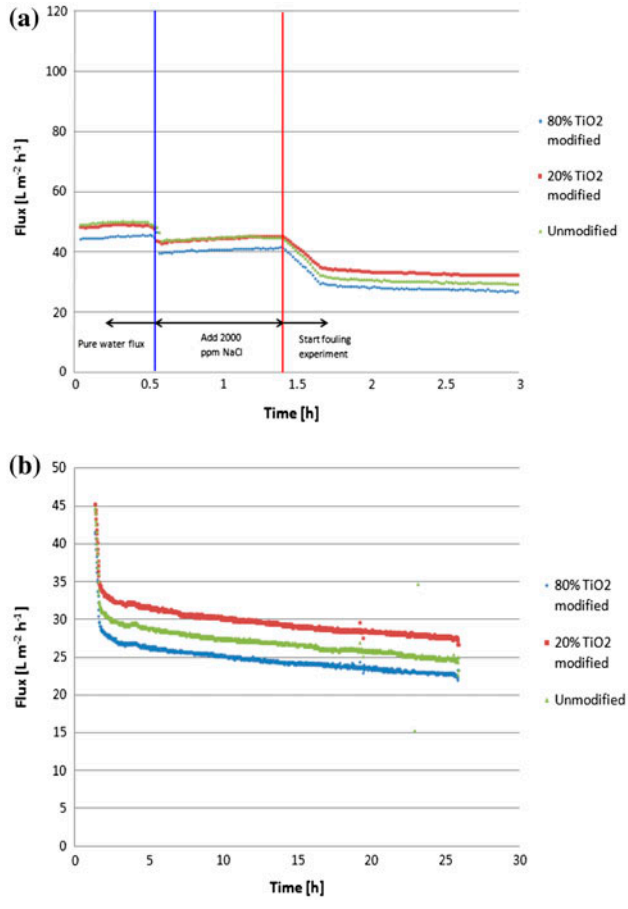

Fig. 8. Permeate flux vs. time (h) for the three selected membranes unmodified, 20 and 80% TiO_2 in organic phase for (a) the first 3 h and (b) for 25 h.

membrane of 20% TiO_2 concentration possesses the highest permeate than both unmodified and 80% TiO_2 PA-TFNC membrane, respectively. This is due to its highest hydrophilicity.

4. Conclusions

This study developed new types of TFNC membranes that containing TiO_2 nanoparticles in the PA thin-film layer. These types were synthesized using *in situ* IP between MPD and TMC. The incorporation of TiO_2 nanoparticles was carried out in either organic or aqueous phase and confirmed by ATR-FTIR, contact angle measurement, SEM, and XPS.

By introduction of TiO_2 nanoparticles in organic phase, the membrane hydrophilicity and flux were enhanced with slightly increase of salt rejection (%) in compared with neat PA/TFC membranes. The water flux from 33.6 to 39.6 ($L/m^2 h$) with slightly improved in salt rejection which increase from 99.75 to 99.83 (%). Also, in case of incorporation of TiO_2 nanoparticles in aqueous phase, the flux increased from 33.6 to 40.16 ($L/m^2 h$) with slight effect in salt rejection. Also, the organic antifouling resistance was studied using three selected membranes and did not show a significant improvement in the organic antifouling resistance but it was expected to improve the bio-antifouling resistance.

Acknowledgments

The author thank Science and Technology Development Fund (STDF) and USA-Egypt Science and Technology collaboration program for supporting his scientific visit in chemical Engineering Dept., Texas University at Austin, Texas, USA. Also, the author thank Prof. Dr Benny Freeman and all members of his group especially Joseph Cook.

References

[1] L.F. Greenlee, D.F. Lawler, B.D. Freeman, B. Marrot, P. Moulin, Reverse osmosis desalination: Water sources, technology, and today's challenges, Water Res. 43 (2009) 2317–2348.
[2] L.Y. Ng, A.W. Mohammad, C.P. Leo, N. Hilal, Polymeric membranes incorporated with metal/metal oxide nanoparticles: A comprehensive review, Desalination 308 (2013) 15–33.
[3] N. Misdan, W.J. Lau, A.F. Ismail, Seawater reverse osmosis (SWRO) desalination by thin-film composite membrane—Current development, challenges and future prospects, Desalination 287 (2012) 228–237.
[4] Y. Wang, J.-H. Kim, K.-H. Choo, Y.-S. Lee, C.-H. Lee, Hydrophilic modification of polypropylene microfiltration membranes by ozone-induced graft polymerization, J. Membr. Sci. 169 (2000) 269–276.
[5] N. Maximous, G. Nakhla, W. Wan, Comparative assessment of hydrophobic and hydrophilic membrane fouling in wastewater applications, J. Membr. Sci. 339 (2009) 93–99.
[6] H.Y. Yu, M.X. Hu, Z.K. Xu, J.L. Wang, S.Y. Wang, Surface modification of polypropylene microporous membranes to improve their antifouling property in MBR: NH plasma treatment, Sep. Purif. Technol. 45 (2005) 8–15.
[7] Q. Sun, Y. Su, X. Ma, Y. Wang, Z. Jiang, Improved antifouling property of zwitterionic ultrafiltration membrane composed of acrylonitrile and sulfobetaine copolymer, J. Membr. Sci. 285 (2006) 299–305.
[8] R. Sheikholeslami, Fouling mitigation in membrane processes, Desalination 123 (1999) 45–53.
[9] A. Asatekin, A. Menniti, S. Kang, M. Elimelech, E. Morgenroth, A.M. Mayes, Antifouling nanofiltration membranes for membrane bioreactors from self-assembling graft copolymers, J. Membr. Sci. 285 (2006) 81–89.
[10] N. Singh, S.M. Husson, B. Zdyrko, I. Luzinov, Surface modification of microporous PVDF membranes by ATRP, J. Membr. Sci. 262 (2005) 81–90.
[11] F.Q. Nie, Z.K. Xu, X.J. Huang, P. Ye, J. Wu, Acrylonitrile-based copolymer membranes containing reactive groups: Surface modification by the immobilization of poly(ethylene glycol) for improving antifouling property and biocompatibility, Langmuir 19 (2003) 9889–9895.
[12] D.S. Wavhal, E.R. Fisher, Membrane surface modification by plasma-induced polymerization of acrylamide for improved surface properties and reduced protein fouling, Langmuir 19 (2003) 79–85.
[13] N.A. Ochoa, M. Masuelli, J. Marchese, Effect of hydrophilicity on fouling of an emulsified oil wastewater with PVDF/PMMA membranes, J. Membr. Sci. 226 (2003) 203–211.
[14] S.P. Nunes, M.L. Sforça, K.V. Peinemann, Dense hydrophilic composite membranes for ultrafiltration, J. Membr. Sci. 106 (1995) 49–56.
[15] K.J. Kim, A.G. Fane, C.J.D. Fell, The performance of ultrafiltration membranes pretreated by polymers, Desalination 70 (1988) 229–249.
[16] M. Khayet, J.P.G. Villaluenga, J.L. Valentin, M.A. López-Manchado, J.I. Mengual, B. Seoane, Filled poly (2,6-dimethyl-1,4-phenylene oxide) dense membranes by silica and silane modified silica nanoparticles: Characterization and application in pervaporation, Polymer 46 (2005) 9881–9891.
[17] J. Du, L. Wu, C.Y. Tao, C.X. Sun, Acta Physico-Chimica Sinica 20 (2004) 598.
[18] A. Bottino, G. Capannelli, A. Comite, Preparation and characterization of novel porous PVDF-ZrO_2 composite membranes, Desalination 146 (2002) 35–40.
[19] C.E.L. Trigo, A.O. Porto, G.M. De Lima, Characterization of CdS nanoparticles in solutions of P(TFE-co-PVDF-co-Prop)/N,N-dimethylformamide, Eur. Polym. J. 40 (2004) 2465–2469.
[20] T.H. Bae, T.M. Tak, Effect of TiO_2 nanoparticles on fouling mitigation of ultrafiltration membranes for activated sludge filtration, J. Membr. Sci. 249 (2005) 1–8.

[21] S.H. Kim, S.Y. Kwak, B.H. Sohn, T.H. Park, Design of TiO_2 nanoparticle self-assembled aromatic polyamide thin-film-composite (TFC) membrane as an approach to solve biofouling problem, J. Membr. Sci. 211 (2003) 157–165.
[22] J. Li, Y. Liang, H. Wang, X. Sun, L. Wang, Acta Polymerica Sinica (2004) 709.
[23] I. Losito, A. Amorisco, F. Palmisano, P.G. Zambonin, X-ray photoelectron spectroscopy characterization of composite TiO_2–poly(vinylidenefluoride) films synthesised for applications in pesticide photocatalytic degradation, Appl. Surf. Sci. 240 (2005) 180–188.
[24] N.-L. Wu, M.-S. Lee, Enhanced TiO_2 photocatalysis by Cu in hydrogen production from aqueous methanol solution, Int. J. Hydrogen Energy 29 (2004) 1601–1605.
[25] M. Keshmiri, M. Mohseni, T. Troczynski, Development of novel TiO_2 sol–gel-derived composite and its photocatalytic activities for trichloroethylene oxidation, Appl. Catal., B 53 (2004) 209–219.
[26] S.H. Kim, S.-Y. Kwak, B.-H. Sohn, T.H. Park, Design of TiO_2 nanoparticle self-assembled aromatic polyamide thin-film-composite (TFC) membrane as an approach to solve biofouling problem, J. Membr. Sci. 211 (2003) 157–165.
[27] Y. Zhao, J. Zhong, H. Li, N. Xu, J. Shi, Fouling and regeneration of ceramic microfiltration membranes in processing acid wastewater containing fine TiO_2 particles, J. Membr. Sci. 208 (2002) 331–341.
[28] S.Y. Kwak, S.H. Kim, S.S. Kim, Hybrid organic/inorganic reverse osmosis (RO) membrane for bactericidal anti-fouling. 1. Preparation and characterization of TiO_2 nanoparticle self-assembled aromatic polyamide thin-film composite (TFC) membrane, Environ. Sci. Technol. 35 (2001) 2388–2394.
[29] G.E. Mitchell, B. Mickols, D. Hernandez-Cruz, A. Hitchcock, Unexpected new phase detected in FT30 type reverse osmosis membranes using scanning transmission X-ray microscopy, Polymer 52 (2011) 3956–3962.
[30] W. Xie, G.M. Geise, B.D. Freeman, H.-S. Lee, G. Byun, J.E. Mcgrath, Polyamide interfacial composite membranes prepared from m-phenylene diamine, trimesoyl chloride and a new disulfonated diamine, J. Membr. Sci. 403–404 (2012) 152–161.
[31] K. Kratz, W. Xie, A. Lee, B.D. Freeman, T. Emrick, Phosphorylcholinesubstituted ROMP polyolefin coatings provide fouling resistance to membrane materials, Macromol. Mater. Eng. 296 (2011) 1142–1148. doi: 10.1002/mame.201100064.
[32] H.S. Lee, S.J. Im, J.H. Kim, H.J. Kim, J.P. Kim, B.R. Min, Polyamide thin-film nanofiltration membranes containing TiO_2 nanoparticles, Desalination 219 (2008) 48–56.
[33] S.J. Lee, S.W. Han, M. Yoon, K. Kim, Adsorption characteristics of 4-dimethylaminobenzoic acid on silver and titania: Diffuse reflectance infrared Fourier transform spectroscopy study, Vib. Spectrosc 24 (2000) 265–275.
[34] S.-Y. Kwak, S.G. Jung, S.H. Kim, Structure-motion-performance relationship of flux-enhanced reverse osmosis (RO) membranes composed of aromatic polyamide thin films, Environ. Sci. Technol. 35 (2001) 4334–4340.
[35] C.E. Reid, E.J. Breton, Water and ion flow across cellulosic membranes, J. Appl. Polym. Sci. 1 (1959) 133–143.
[36] S. Scheiner, Hydrogen Bonding: A Theoretical Perspective, Oxford University Press, Oxford, NY, 1997.